Description of Phase Behavior of Polymer Blends by Different Equation-of-State Theories. 1. Phase Diagrams and Thermodynamic Reasons for Mixing and Demixing

Bernd Rudolf* and Hans-Joachim Cantow

Freiburger Materialforschungszentrum (FMF) und Institut für Makromolekulare Chemie, Albert-Ludwigs-Universität, Stefan-Meier-Strasse 21, 79104 Freiburg, Germany

Received October 13, 1994; Revised Manuscript Received May 31, 1995[⊗]

ABSTRACT: A comparison has been made between the Sanchez−Lacombe equation-of-state theory and the theory of Patterson for describing the phase behavior of various polymer blends. Phase diagrams have been determined as well as PVT data, in order to determine the reduction parameters of the polymers used. With these data the phase diagrams were simulated applying these two theories. Furthermore, the cause of compatibility or incompatibility, i.e., the influence of free volume and enthalpic effects were investigated. Both theories show surprisingly similar behavior with respect to the mentioned properties.

Introduction

There are a number of thermodynamic theories that describe polymer liquids and also polymer blends. The first one which was developed is the well-known Flory−Huggins theory.[1] It is a rigid lattice model that ignores free volume. Therefore, this simple model could not account for many observed effects such as volume change upon mixing or lower critical solution temperature (LCST) behavior. Various theories have been presented that allow for the possibility of volume changes. The first one presented for chain molecules is due to Prigogine et al.[2] It is a cell model theory with a configurational partition function based on the Hirschfelder−Eyring partition function.[3] A hard-sphere repulsive potential is assumed for the segments of the polymer chain moving in a square-well potential, thus introducing a free volume. From this theory an equation-of-state (EOS) can be derived that obeys a principle of corresponding states. A modified version of this theory has been given by Flory et al.,[4,5] the main difference being the replacement of the generalized Lennard-Jones potential by a van der Waals type potential. We will refer to this model as the Prigogine−Flory (PF) theory. It is the most extensively used theory nowadays.

On the basis of the Prigogine corresponding states theory, Patterson[6] derived a simpler EOS theory which is formally identical with the Flory−Huggins theory but whose interaction parameter also contains EOS contributions. We will call this theory the PF−Patterson (PFP) theory.

Another EOS theory is the lattice-fluid theory due to Sanchez and Lacombe.[7,8] Formally it is similar to the Flory−Huggins theory, but a free-volume term is introduced via vacant lattice sites. The EOS derived from this theory does not strictly satisfy a principle of corresponding states.

Theory

PF−Patterson theory. In the PF theory, the quantities characterizing a liquid are the reduction parameters p^*, v_s^*, and T^*. They can be used to express the reduced pressure, volume, and temperature, defined by

$$\tilde{p} = \frac{p}{p^*} \qquad \tilde{v} = \frac{v_s}{v_s^*} = \frac{v}{v^*} \qquad \tilde{T} = \frac{T}{T^*} \tag{1}$$

v_s is the specific volume, i.e., the reciprocal of the mass density. v_s^* is the specific "hard-core volume", i.e., the specific volumes at 0 K; v and v^* are the volume and hard-core volume of a polymer-segment. These reduced quantities are linked by the EOS, which for the PF theory is given by

$$\frac{\tilde{p}\tilde{v}}{\tilde{T}} = \frac{\tilde{v}^{1/3}}{\tilde{v}^{1/3} - 1} - \frac{1}{\tilde{v}\tilde{T}} \tag{2}$$

This allows the quantities $\tilde{v}$ and $\tilde{T}$, and hence v_s^* and T^*, to be calculated from the thermal expansion coefficient α and the specific volume at $p = 0$:

$$\tilde{v}^{1/3} - 1 = \alpha T/3(1 + \alpha T) \tag{3}$$

$$\tilde{T} = (\tilde{v}^{1/3} - 1)/\tilde{v}^{4/3} \tag{4}$$

Both $\tilde{v}$ and $\tilde{T}$ are a measure of free volume.

The reduction pressure p^* is obtained from

$$p^* = \frac{\alpha}{\kappa}\tilde{v}^2 T \tag{5}$$

with the compressibility κ at $p = 0$.

For polymer mixtures formally the same expressions result, where the quantities p^* and T^* of the mixtures are linked to those of the pure components, and an additional parameter X_{12}, the contact energy parameter, occurs. The size of the hard-core volumes for a segment can be chosen arbitrarily. For the mixture they are set equal for both components, $v_1^* = v_2^* = v^*$. We chose the geometric mean of the value of the two monomeric units.

An expression for the interaction parameter χ has been derived by Patterson for zero pressure from the Prigogine corresponding states theory. It contains contact energy and free volume contributions:

$$\chi = -\frac{U_1 \nu^2}{RT} + \frac{C_{p1}}{2R}\tau^2 \tag{6}$$

U_1 is the internal energy of component 1, ν^2 is a measure of the relative weakness of the (1−2) contact to the

[⊗] Abstract published in *Advance ACS Abstracts,* August 1, 1995.

0024-9297/95/2228-6586$09.00/0

average of (1−1) and (2−2) contacts, and C_{p1} the constant pressure heat capacity of component 1. Equation 6 is quite general. To be able to give explicit expressions for the quantities appearing in the expression for χ, a particular model has to be applied.

In the PF model U_1 is given by

$$-U_1 = p^*_1 V^*_1 / \tilde{v}_1 \tag{7}$$

with the molar hard-core volume V^*. ν^2 reads

$$\nu^2 = X_{12}/p^*_1 \tag{8}$$

with the contact energy parameter X_{12} of the PF theory. Furthermore one obtains

$$C_{p1} = p^*_1 V^*_1 \tilde{v}_1^{1/3} / T^*_1 (^4/_3 - \tilde{v}_1^{1/3}) \tag{9}$$

τ is given by

$$\tau = 1 - \frac{T^*_1}{T^*_2} \tag{10}$$

It is a measure of the free-volume difference between the two components. The first term of eq 6 represents the interactional part, the second the free volume part of the χ-parameter.

The spinodals and binodals are calculated using the expression known from Flory−Huggins theory. The condition for phase stability of a binary system reads

$$2\chi < \frac{1}{r_1\Phi_1} + \frac{1}{r_2\Phi_2} \tag{11}$$

with the number r_i of segments per chain of component i, and the corresponding volume fraction Φ_i. (The segment and surface fractions appearing in the PF theory are set equal to the volume fractions.)

Sanchez−Lacombe Theory. The Sanchez−Lacombe (SL) theory is a lattice theory that also includes vacant lattice sites. A binary system is formally treated as a three-component system, where the third component is represented by the holes. The theory is similar to the Flory−Huggins treatment of ternary systems, but hole−hole and hole−mer interactions are assigned a zero energy, so that there remains only one interaction parameter χ_{SL}, as one expects for a binary system. As in the PF or in the PFP theory, a liquid (i.e., both pure liquids and mixtures) is characterized by three reduction parameters p^*, v_s^*, and T^*. Again v_s^* is the specific hard-core volume, which in this case means the specific volume of the occupied lattice sites. Reduced quantities can be defined analogously to those in eq 1:

$$\tilde{p} = \frac{p}{p^*} \qquad \tilde{v} = \frac{v_s}{v_s^*} = \frac{N_0 + rN}{rN} \qquad \tilde{T} = \frac{T}{T^*} \tag{12}$$

with the number N_0 of vacancies, and $rN = r_1N_1 + r_2N_2$ of occupied lattice sites. N_i is the number of molecules of component i, r_i the corresponding number of mers per chain, and $N = N_1 + N_2$ the total number of polymer chains.

Again, the quantities p^* and T^* of a mixture are related to those of the pure components, and the interaction parameter χ_{SL}. However, in contrast to other lattice theories, in the SL theory, the volume v^* of a lattice site is fixed and cannot be chosen arbitrarily. The size of the site for a mixture is an average of those of the pure components, and depends on composition. Hence, the number r_i of lattice sites occupied by one molecule in the mixture also differs from the number r_i^0 of occupied sites in the pure system. r_i proves to be about 5−10 times larger than the degree of polymerization, i.e., the volume of a lattice site is smaller by this factor. The EOS of this model is given by

$$\frac{1}{\tilde{v}^2} + \tilde{p} + \tilde{T}\left[\ln\left(1 - \frac{1}{\tilde{v}}\right) + \left(1 - \frac{1}{r}\right)\frac{1}{\tilde{v}}\right] = 0 \tag{13}$$

which again holds for one-component systems, as well as for mixtures.

In contrast to the EOS of the PF theory, this equation depends on the chain length r, i.e., it does not satisfy a principle of corresponding states. Only in the limit $r \to \infty$ a principle of corresponding states is valid. For mixtures, r is an average chain length given by

$$r = \frac{N_1 r_1 + N_2 r_2}{N_1 + N_2} \tag{14}$$

For vanishing pressure and infinite chain length the reduced variables $\tilde{v}$ and $\tilde{T}$ can be determined from the EOS and the thermal expansion coefficient for $p = 0$:

$$\frac{1}{\tilde{v}^2} + \tilde{T}\left[\ln\left(1 - \frac{1}{\tilde{v}}\right) + \frac{1}{\tilde{v}}\right] = 0 \tag{15}$$

$$\alpha T = \frac{1}{\tilde{T}/(1 - 1/\tilde{v}) - 2} \tag{16}$$

However, these equations cannot be solved explicitly for the desired variables, so they have to be solved numerically. The parameter p^* is obtained from

$$p^* = \frac{\alpha}{\kappa}\tilde{v}^2 T \tag{17}$$

The intermolecular energy E of such a system can be expressed as

$$E = -rN\frac{\epsilon^*}{\tilde{v}} \tag{18}$$

with

$$\epsilon^* = \Phi_1\epsilon^*_{11} + \Phi_2\epsilon^*_{22} - \Phi_1\Phi_2 kT\chi_{SL} \tag{19}$$

and

$$\chi_{SL} = (\epsilon^*_{11} + \epsilon^*_{22} - 2\epsilon^*_{12})/kT \tag{20}$$

where ϵ^*_{ij} is the mean interaction energy of a mer of component i with its neighbouring mer of component j. χ_{SL} is the analogue of the χ parameter of the original Flory−Huggins theory or of X_{12} in the Flory−Prigogine theory.

The combinatorial entropy is simlar to the Flory−Huggins expression for a ternary system composed of two polymers and solvent:

$$S = -k(N_0 + Nr)\left[f_0 \ln f_0 + \frac{f_1}{r_1}\ln\left(\frac{f_1}{\omega_1}\right) + \frac{f_2}{r_2}\ln\left(\frac{f_2}{\omega_2}\right)\right] \tag{21}$$

f_0 is the fraction of empty sites, f_i the fraction of sites occupied by component i, and ω_i the number of configurations available to an r_i-mer. Expressed by the hard-core volume fractions (or segment fractions) Φ_1 and Φ_2

of the two components, this yields

$$S = -kNr\left[\frac{\Phi_1}{r_1}\ln\left(\frac{\Phi_1}{\omega_1}\right) + \frac{\Phi_2}{r_2}\ln\left(\frac{\Phi_2}{\omega_2}\right) + (\tilde{v}-1)\ln\left(1-\frac{1}{\tilde{v}}\right) - \frac{1}{r}\ln\tilde{v}\right] \quad (22)$$

As for the PFP theory we will identify the segment fractions with the volume fractions, in order to be able to compare the calculated with the experimental composition variables.

The first two terms of eq 22 correspond to the well-known Flory–Huggins combinatorial entropy, whereas the others are due to the presence of vacancies. The latter two terms and the $1/\tilde{v}$ dependence of the energy in eq 18 introduce the volume-dependence into the free energy. Beside the EOS, the spinodal condition and the chemical potentials can be deduced from this.

For vanishing pressure, the spinodal condition obtained from this theory is given by

$$\frac{1}{\tilde{v}}\{2[(\Phi_1 + \nu\Phi_2)\chi_{SL} + (1-\nu)\lambda_{12}] + \tilde{T}\Psi^2 p^*\kappa(\Phi_1 + \nu\Phi_2)\} = \frac{1}{r_1^0\Phi_1} + \frac{\nu}{r_2^0\Phi_2} \quad (23)$$

with

$$\lambda_{12} = \frac{1}{\tilde{T}_1} - \frac{1}{\tilde{T}_2} + (\Phi_1 - \Phi_2)\chi_{SL} \quad (24)$$

$$\Psi = \frac{\lambda_{12}}{\tilde{v}} - \frac{\nu}{(\Phi_1 + \nu\Phi_2)^2}\left(\frac{1}{r_1^0} - \frac{1}{r_2^0}\right) \quad (25)$$

and the ratio

$$\nu = v^*_1/v^*_2 \quad (26)$$

which for $\nu \neq 1$ corresponds to the introduction of a surface area effect.[8] The chemical potential of component 1 reads

$$\mu_1 = kT\left\{\ln\Phi_1 + \left(1-\frac{r_1}{r_2}\right)\Phi_2 + \frac{r_1^0}{\tilde{v}}[\chi_{SL} + (1-\nu)\lambda_{12}]\Phi_2^2 + r_1^0 kT^*_1\left\{-\frac{1}{\tilde{v}} + \tilde{T}_1\left[(\tilde{v}-1)\ln\left(1-\frac{1}{\tilde{v}}\right) - \frac{1}{r_1^0}\ln(\tilde{v}\omega_1)\right]\right\}\right\} \quad (27)$$

The chemical potential for component 2 is obtained by appropriate substitution of indexes.

Experimental Section

Materials. The systems investigated and the characterization of their polymers are given in Table 1. The polymers used were polystyrene (PS), polyisoprene (PI), poly(methylphenylsiloxane) (PMPS), and poly(cyclohexyl methacrylate) (PCHMA). Determination of the reduction parameters will be discussed below.

PVT Measurements. The PVT measurements were performed with a Gnomix-PVT-apparatus (Boulder, CO) whose sample cell contains about 1 g of sample and mercury as a confining fluid. Flexible bellows seal one end of the cell, and the movement of the bellows on changing temperature or pressure is used to calculate the volume change of the sample. The Gnomix apparatus permits PVT measurements in the temperature range between room temperature and 400 °C, and pressures ranging from 10 to 200 MPa. Details are described in the literature.[9]

Table 1. Investigated Systems and the Characterization of Their Polymers

	components	M_n [g/mol]	M_w/M_n
system 1	PS 2.1	2117	1.08
	PI 2.6[a]	2594	1.08
system 2	PS 6	5966	1.12
	PMPS 1.7	1682[b]	1.35[b]
system 3	PS 230	230000	1.11
	PCHMA 114[c]	80740	1.26
		114000[d]	

[a] Anionic polymerization in cyclohexane, initiator *sec*-butyllithium, 90% cis 1,4 contents. [b] Aldrich. [c] Anionic polymerization in THF, initiator 1,1-diphenyl-3-methylpentyllithium. [d] From membrane osmosis.

Table 2. Reduction Parameters of the PF Theory

	p^* [MPa]	v_s^* [cm³/g]	T^* [K]
PS 2.1	559.1	0.8141	7090
PS 6	566.8	0.8436	7728
PS 230	522.6	0.8356	8508
PI 2.6	469.7	0.9396	6713
PMPS 1.7	519.3	0.7583	6459
PCHMA 114	511.4	0.7791	8115

Table 3. Reduction Parameters of the SL Theory

	p^* [MPa]	v_s^* [cm³/g]	T^* [K]
PS 2.1	464.5	0.8996	661.4
PS 6	468	0.9282	715.2
PS 230	428.1	0.9232	796.3
PI 2.6	383	1.0405	631.2
PMPS 1.7	427.65	0.8389	606.7
PCHMA 114	417.6	0.862	760.8

The PVT measurements were performed in the isothermal mode, i.e., the sample was held at a certain temperature, and the pressure was raised from 10 to 200 MPa in steps of 10 MPa. The volume changes corresponding to those pressures were recorded. In addition, the value corresponding to $p = 0$ was extrapolated from these data via the Tait equation. Subsequently this procedure was repeated for other temperatures.

PVT measurements were not performed for PS 230. Instead, the PVT data of a polystyrene of molecular mass M_n = 102 000 and M_w/M_n = 1.05 (PS 102) were used.

Determination of the Parameters of the System. The reduction parameters for both models were determined at $p = 0$ according to eqs 3–5 and eqs 15–17, respectively. The expansion coefficient α was calculated from PVT measurements, and averaged over the temperature range of interest, i.e., the temperature where both components of the system were above their glass transition. For system 1 this was from 80 to 160 °C, for system 2 from 100 to 150 °C, and for system 3 from 150 to 280 °C. The specific volume and the compressibility κ were taken from the isothermal PVT measurements. In this way the reduction parameters were calculated for the same temperature range as α. Since they turn out to be temperature dependent, they were averaged over this temperature range.

As one expects, the coefficients of expansion and the compressibilities of the low molecular weight polystyrenes turn out to be greater than those of the polystyrenes with higher molecular weight. Therefore, their reduction parameters have to be determined separately. The parameters obtained for the PF and the SL theory are given in Tables 2 and 3, respectively.

Cloud-Point Determination. The PS/PI blends were prepared by dissolving in tetrahydrofuran, precipitating with an excess of methanol, and filtering. Subsequently the blends were dried in a vacuum oven for 3 days at 50 °C.

For the cloud-point determination, the samples were filled between two quartz glass sheets, which were sealed with a rubber ring.

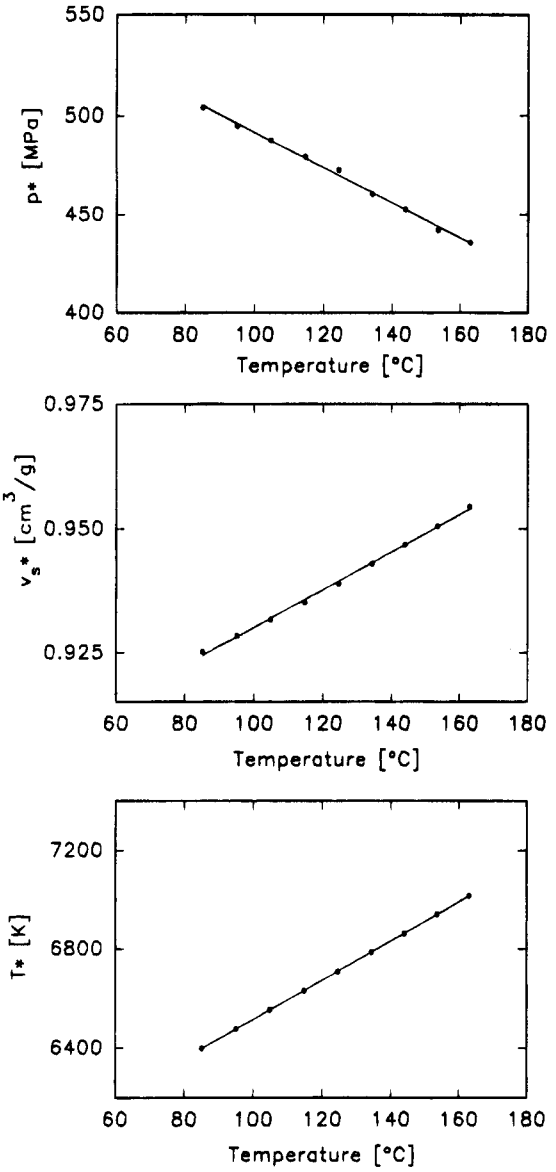

Figure 1. Reduction parameters of PI 2.6 for the PF theory as a function of temperature.

Since the PMPS has a very low viscosity, the PS/PMPS blends could be prepared by directly dissolving the PS in PMPS at 150 °C. At that temperature, the blends were clear and became turbid upon cooling.

The preparation for the cloud-point determination was done in the same way as for PS/PI.

The PS/PCHMA blends were prepared by casting films from a solution in tetrahydrofuran. The films were brought between two quartz glass sheets for the cloud-point measurements.

The cloud-points were determined by repeated heating and cooling of the samples with decreasing rates and visual inspection. In this way, the cloud-point temperatures could be approached gradually. For the PS/PCHMA blends, an additional annealing at each temperature was necessary.

Results and Discussion

As mentioned above, the reduction parameters are found to be functions of temperature. The reduction pressure p^* decreases with increasing temperature, whereas the reduction volume and the reduction temperature increase. This is true for both models. In Figure 1 the reduction parameters of PI 2.6 for the PF theory are shown as a function of temperature. The parameters for the SL theory have different numerical values, but they exhibit the same principle behavior.

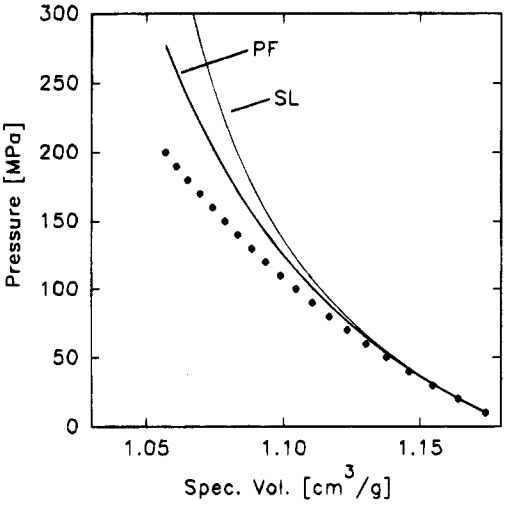

Figure 2. Pressure vs specific volume for PI 2.6. The dots represent experimental values, the lines are calculated according to the two theories.

Figure 2 shows pressure vs specific volume for the same polymer at 125 °C. The dots represent experimental values, and the lines show the values calculated from the equations-of-state for the two models. It can be seen that for low pressures, agreement between calculated and experimental values is fairly good. For higher pressures however, the calculated curves deviate significantly from the experimental points. The deviation is much greater for the SL theory than for the PF theory. For a given volume, the pressure predicted by the models is too high, i.e., the compressibilities would be too low. This indicates, that the free volume predicted by the two models is too small, the value obtained by the SL theory is even smaller than that given by the PF theory.

Since the chain length r enters into the EOS of the SL theory, it also appears in the coefficient of expansion. The theory predicts at least qualitatively correct higher values for α of low molecular weight polymers and oligomers than for the corresponding high molecular weight polymers. So in principle, it should be sufficient to determine the parameters of a given polymer, and one would know the parameters for all chain lengths. However, the predicted increase of α with decreasing molecular weight is too low. This means that the reduction parameters for the low molecular weight polystyrenes have to be determined separately, as for the PF theory. In Figure 3, the expansion coefficient of polystyrene is shown as a function of molecular weight at 150 °C. The line is calculated by using the parameters from PS 102, the dots are experimental data. The experimental value of α for PS 102 does not coincide exactly with the calculated one. This is due to the fact that the theory predicts an increase of α with increasing temperature, whereas the calculation was performed using an averaged value.

The experimental phase diagrams of the three systems are shown in Figure 4. The dots represent the experimental values, the lines are drawn to guide the eye.

The phase diagram of PS/PMPS could not be determined for high concentrations of PS, because during cooling of the homogeneously mixed blend, the glass transition occurred before demixing. Therefore, the homogeneous state was frozen in.

Model Calculations. To be able to carry out the simulations, knowledge of the interaction energy of the

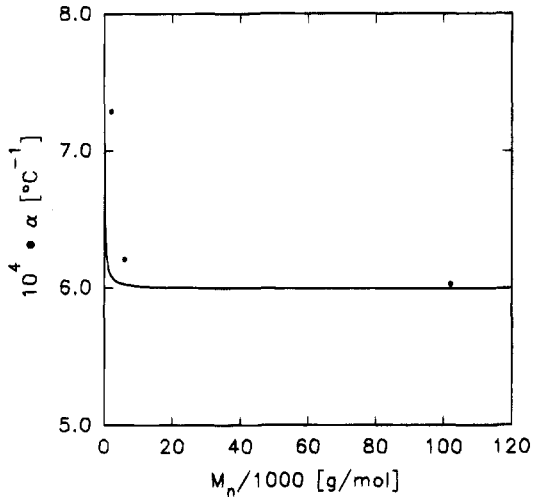

Figure 3. Expansion coefficient for polystyrene as a function of molecular weight. The dots are experimental, the line is calculated with the SL theory using the data of PS 102.

hetero contacts is required in addition to the interaction energy of the homo contacts. The simplest approach would be to adopt the familiar Berthelot relationship:

$$\epsilon_{12} = (\epsilon_{11}\epsilon_{22})^{1/2} \tag{28}$$

It would then be sufficient to have knowledge of only the pure blend components. However, this does not give an adequate description of the observed phenomena. Another possibility to obtain the required parameters would be from PVT data of the blends, i.e., from their reduction parameters. However, it appears that the results obtained from blend data strongly depend on composition, and even different results are obtained by determination from the parameters p^* or T^*.

There are still other methods for estimating this parameters, but the only satisfactory procedure is to fit it to experiment. Equivalently, X_{12} or χ_{SL} respectively can be adapted.

Introducing the Berthelot relationship into the PFP theory yields for X_{12}

$$X_{12} = p^*_1\left[1 - \left(\frac{p^*_2}{p^*_1}\right)^{1/2}\right]^2 \tag{29}$$

Sanchez and Lacombe adopted the Berthelot relationship for their theory. But since this relationship fails in most cases, they introduced a parameter ζ which is a measure of the deviation from this relationship. Then, instead of fitting χ_{SL}, SL determined the parameter ζ from experiment:

$$\zeta = \epsilon^*_{12}/(\epsilon^*_{11}\epsilon^*_{22})^{1/2} \tag{30}$$

$\zeta \leq 1$ means that χ_{SL} is positive, for $\zeta > 1$ χ_{SL} can be positive or negative.

Calculation of Phase Diagrams. The phase diagram of the system PS/PI calculated with the PFP theory and assuming the validity of eq 28 is shown in Figure 5a. The theory predicts at least qualitatively correctly the UCST behavior. The phase diagram of this system calculated with the SL theory is shown in Figure 5b. ζ was set equal to 1, i.e., no adaption of the parameter was necessary either, to obtain a UCST-type phase diagram. The critical temperature is predicted fairly well by this model.

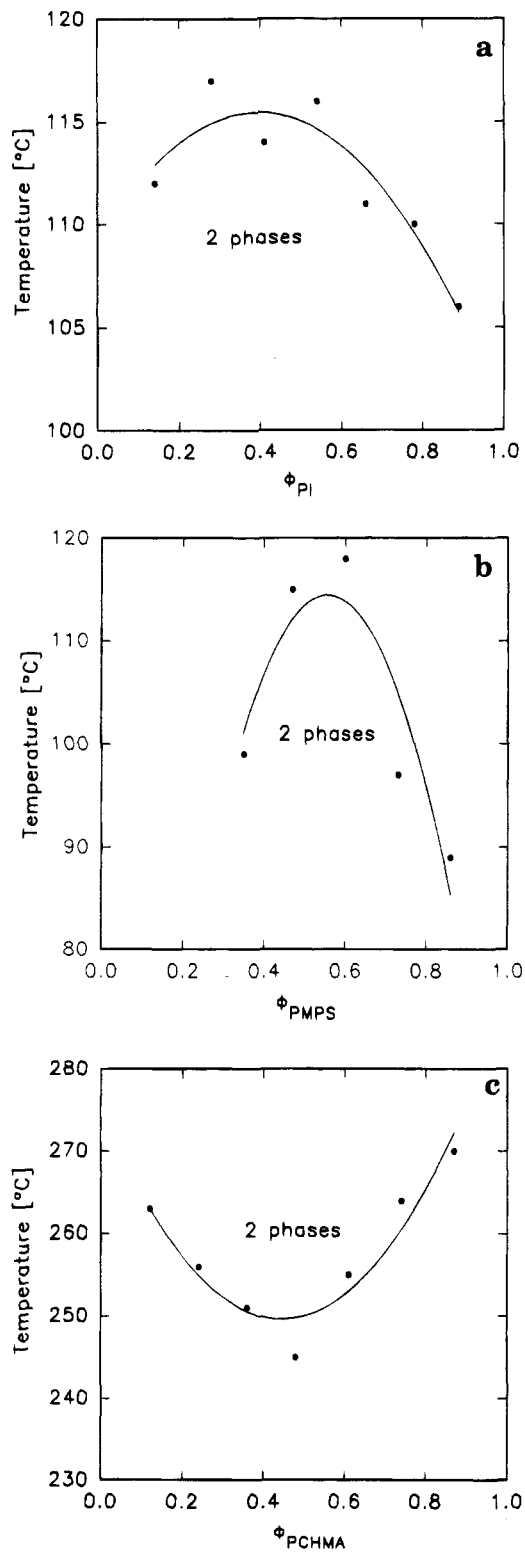

Figure 4. Cloud points of the systems investigated: (a) PS/PI; (b) PS/PMPS; (c) PS/PCHMA.

For the blend system PS/PMPS, the Berthelot relationship fails. Calculating X_{12} from blend data, one finds that different compositions yield different values. Even for the same blend, the X_{12} values obtained from p^* and T^* are different. Such inconsistencies have already been observed before.[10]

Therefore, this parameter has to be fitted to the experiment. However, it is not possible to adapt it in such a way, that the critical temperature is in accordance with the experimental phase diagram. With

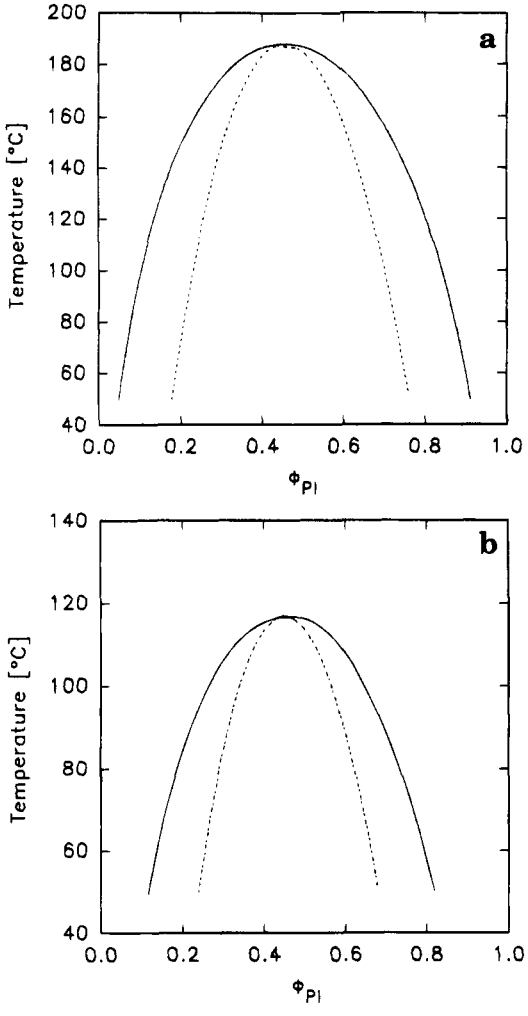

Figure 5. Calculated binodal and spinodal for PS/PI: (a) PFP theory; (b) SL theory.

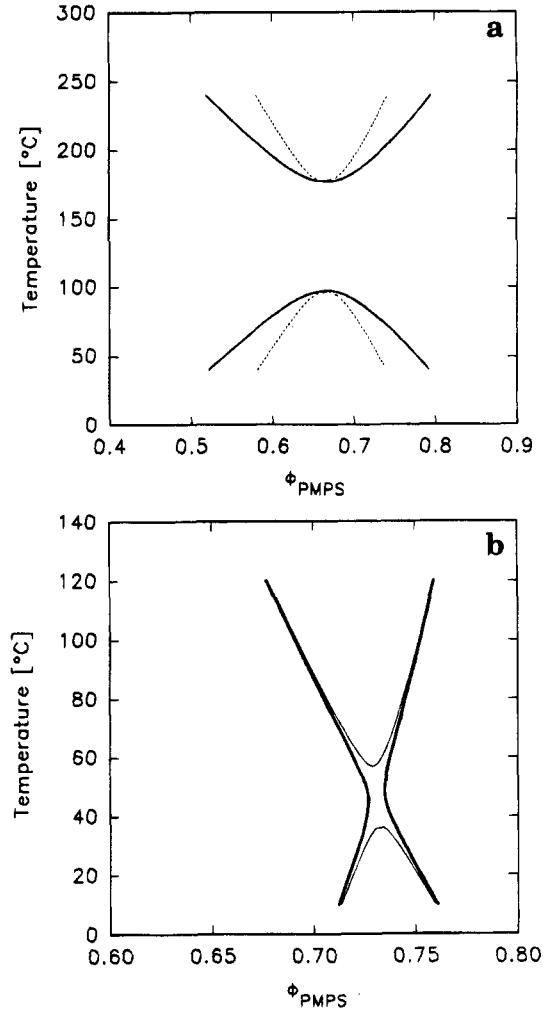

Figure 6. Calculated binodal and spinodal for PS/PMPS: (a) PFP theory; (b) SL theory.

$X_{12} = 1$ J/cm^3, the calculated UCST is about 20 °C below the experimental one. However, with this parameter, the theory predicts not only UCST but also LCST behavior. The corresponding phase diagram calculated with the PFP theory is shown in Figure 6a. If X_{12} is increased in order to get a calculated phase diagram which conforms more closely to the experimental one, the LCST is lowered simultaneously, i.e., UCST and LCST approach each other. Finally, an hourglass-shaped phase diagram results.

The assumed value for X_{12} seems to be reasonable. The values found in the literature[11-13] are of the same order of magnitude.

With the SL theory the situation is quite similar. Again a parameter adaption is required. $\zeta = 1$ would predict complete miscibility for this system. As in the case of the PFP theory, it is not possible to get experimental and calculated critical temperatures into agreement. Again one obtains a phase diagram that shows both, UCST and LCST behavior. Upon a corresponding variation of ζ, they approach each other until they coincide. The shape of the phase diagram depends very sensitively on ζ. This is demonstrated in Figure 6b, where the calculated spinodals are shown for two different values of ζ. For $\zeta = 0.996\,294$ one obtains UCST and LCST behavior (thin lines), $\zeta = 0.996\,293$ yields an hourglass-shaped phase diagram (bold lines).

The system PS/PCHMA exhibits LCST behavior, its description with the PFP theory requires a negative interaction parameter. Again, determination from blends yields entirely different parameters, most of them are positive. So, this parameter also has to be fitted to experiment. The Patterson phase diagram calculated with $X_{12} = -0.1$ J/cm^3 is shown in Figure 7a. The theory predicts a better miscibility on the PS-rich side, i.e., the component with the longer chains. This is what is generally predicted by a Flory–Huggins type theory. Experimentally however, an opposite behavior is observed, the asymmetry of the experimental and calculated phase diagrams disagree.

The corresponding phase diagram calculated with the SL theory is shown in Figure 7b, with $\zeta = 0.999\,890\,6$, corresponding to a positive χ_{SL}. Again, the asymmetry of the calculated phase diagram is at variance with the experimental one.

However, there are also EOS theories that predict phase diagrams with an asymmetry contrary to the one predicted by the two models described here. This has been shown, with the modified cell model (MCM) due to Dee and Walsh[14] for the system polystyrene/poly(vinyl methyl ether).[13]

Discussion of the Phenomena of Demixing. The stability condition, of the PFP theory is given by

$$2(\chi_i + \chi_f) < \frac{1}{r_1\Phi_1} + \frac{1}{r_2\Phi_2} \tag{31}$$

where χ_i and χ_f represent respectively the interactional and the free volume part of the χ parameter.

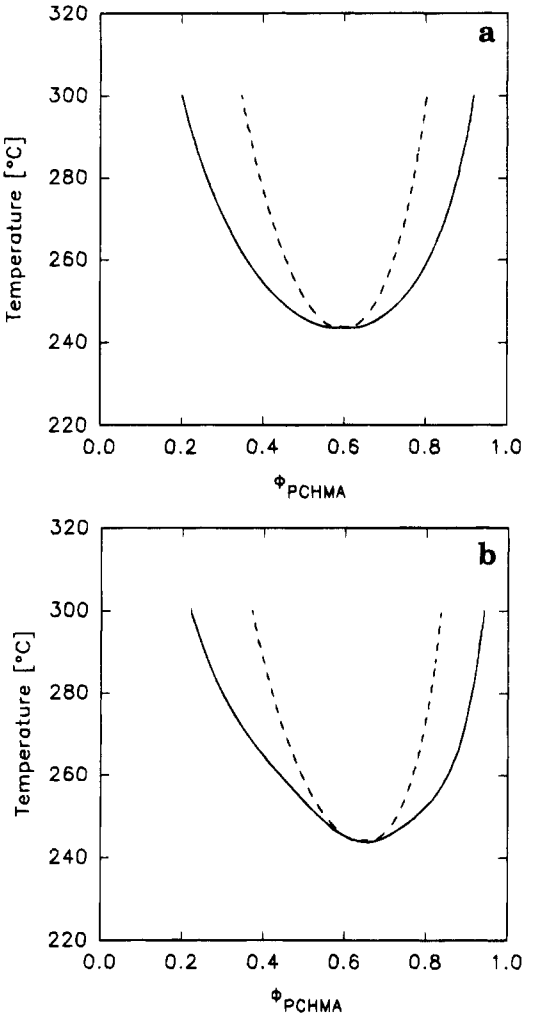

Figure 7. Calculated binodal and spinodal for PS/PCHMA: (a) PFP theory; (b) SL theory.

The stability condition for the SL theory can be formulated similarly. By analogy with the χ parameter of the PFP theory, a parameter Λ consisting of three parts can be defined:

$$\Lambda = \Lambda_\chi + \Lambda_f + \Lambda_s \tag{32}$$

with

$$\Lambda_\chi = \frac{1}{\tilde{v}}(\Phi_1 + \nu\Phi_2)\chi_{SL}$$

$$\Lambda_f = \frac{1}{2\tilde{v}}\tilde{T}\Psi^2 p^* \kappa(\Phi_1 + \nu\Phi_2) \tag{33}$$

$$\Lambda_s = \frac{1}{\tilde{v}}(1 - \nu)\lambda_{12}$$

The stability condition then has the form

$$2\Lambda < \frac{1}{r_1^0\Phi_1} + \frac{\nu}{r_2^0\Phi_2} \tag{34}$$

The first term Λ_χ is an interactional term, the second term Λ_f is due to the introduction of free volume, and Λ_s arises from the surface area effect; hence it is also an interactional term. From the temperature dependence of λ_{12} and χ_{SL}, one can see that both interactional terms have the same temperature dependence, they are proportional to $1/(\tilde{v}T)$. This is the same temperature dependence that is exhibited by the interactional term of the PFP theory. However, in contrast to the χ parameter of the PFP theory, the parameter Λ depends on composition and via the reduced volumes also on the chain lengths of the components.

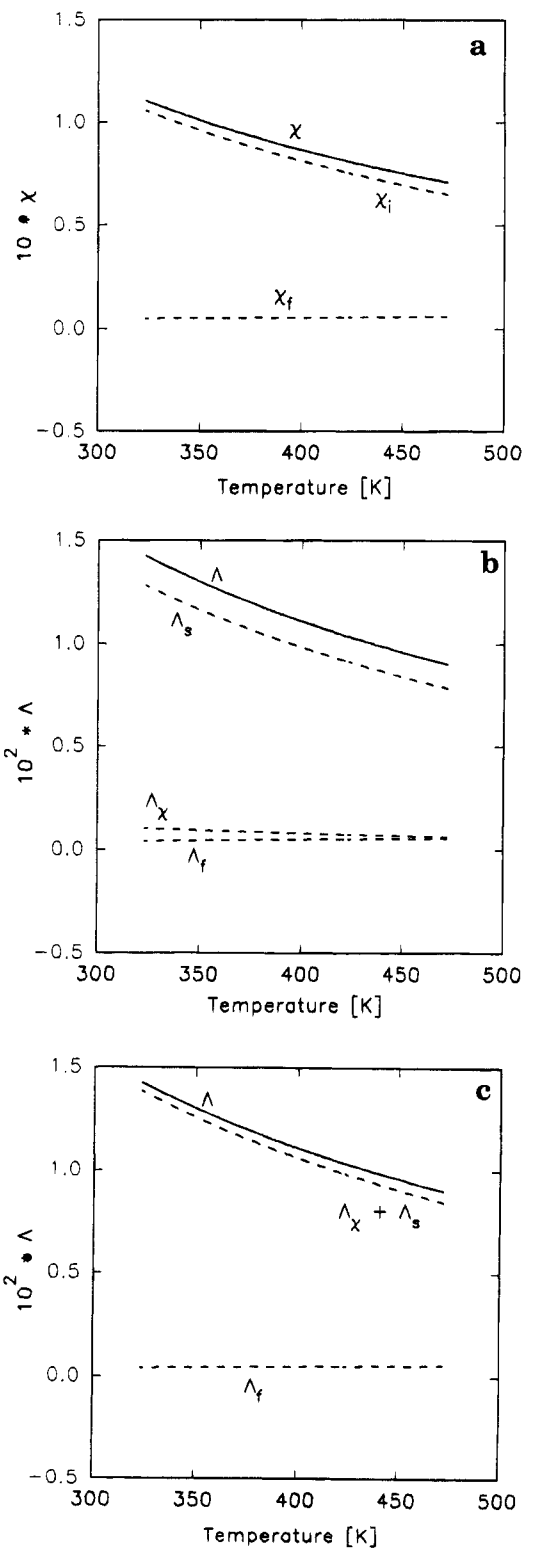

Figure 8. Temperature dependence of the various contributions of the interaction parameter of PS/PI: (a) χ; (b) Λ; (c) Λ (interactional terms combined).

Figure 8a shows the calculated Patterson χ parameter for PS/PI as a function of temperature. Its free volume part is virtually independent of temperature and very small, so that the behavior is governed by the interactional part. The latter decreases as the temperature is

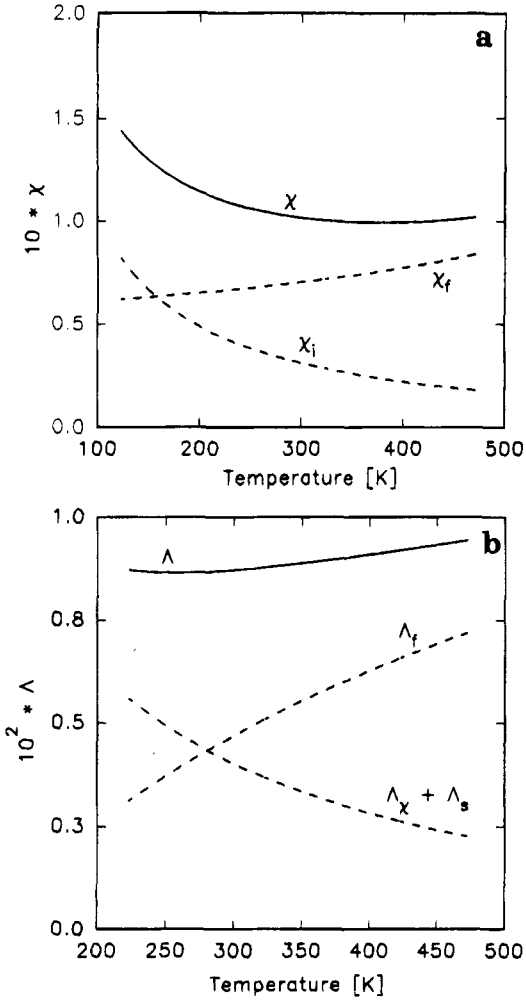

Figure 9. Temperature dependence of the various contributions of the interaction parameter of PS/PMPS: (a) χ; (b) Λ (interactional terms combined).

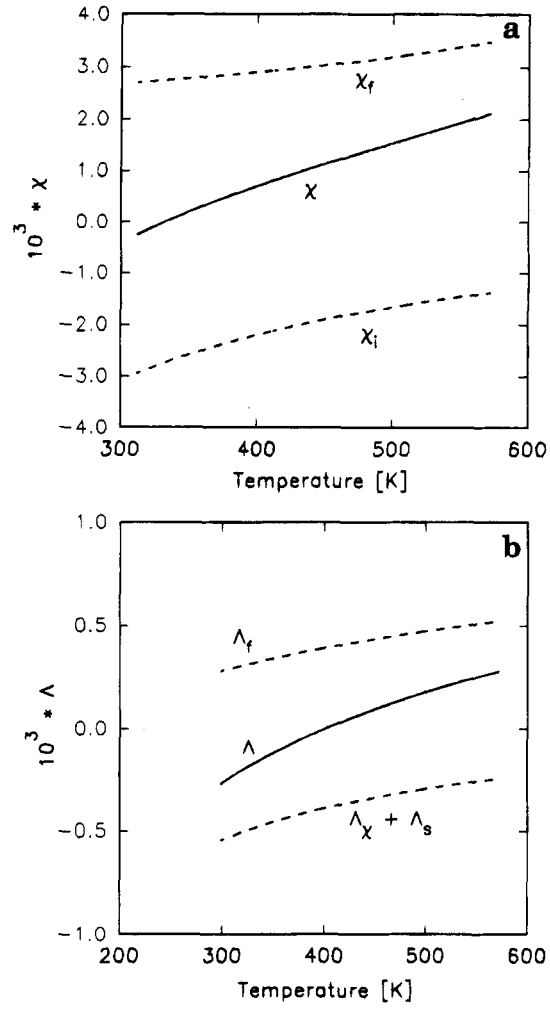

Figure 10. Temperature dependence of the various contributions of the interaction parameter of PS/PCHMA: (a) χ; (b) Λ (interactional terms combined).

increased, thus favoring miscibility and resulting in UCST behavior.

In Figure 8b the three parts of the parameter Λ and the overall parameter of PS/PI are shown as a function of temperature for $\Phi_{PI} = 0.5$. The free-volume part is very small and hardly varies with temperature, similar to Λ_χ. The behavior is governed by Λ_s, so it is dominated by the interactional terms. The addition of the interactional terms yields curves that are surprisingly similar to the Patterson χ parameter. This is shown in Figure 8c. The difference in the order of magnitude of the χ parameter and the parameter Λ is due to the fact, that they refer to different sizes of the lattice sites.

Λ varies with composition, it decreases with increasing concentration of PI. This means, that the miscibility on the PI rich side of the phase diagram is improved, thus shifting the phase diagram toward the PS side.

The χ parameter of the system PS/PMPS is governed by both the interactional and the free-volume part. At ordinary temperatures, the interactional part is smaller than the free-volume part, but at very low temperatures interactions dominate the behavior. This results in an overall χ parameter, which first decreases but then again increases with increasing temperature (Figure 9a). Thus, UCST and LCST behavior are predicted, as was shown above.

The temperature dependence of Λ of PS/PMPS for $\Phi_{PMPS} = 0.5$ is shown in Figure 9b (interactional terms combined). This was calculated with $\zeta = 0.996\,294$, the value corresponding to the prediction of UCST and LCST. Again one obtains a behavior similar to the PFP theory, i.e., for low temperatures the interactional part dominates, whereas for higher temperatures the free-volume term is dominating.

For this system, Λ also varies with composition. It increases with increasing concentration of PMPS, thus shifting the phase diagram more to the PMPS-rich side, compared to the PFP theory.

The χ parameter for PS/PCHMA is shown in Figure 10a. Its interactional part is—as one expects for a compatible system—negative. Both the interactional and the free-volume part increase upon heating. Hence, the observed miscibility gap is not only an effect of free volume but also a consequence of the weakening of the interactions favoring miscibility. It is interesting to note, that the overall χ parameter determined in this way is positive over most of the temperature range. Direct determination from a phase diagram yields a negative value even at 180 °C.[15]

The interactional term Λ_χ of this system is positive, due to the positive χ_{SL}. However, the negative surface term Λ_s favors miscibility and dominates Λ_χ, so that the overall interactional part compensates the unfavorable free volume term. The sum of the interactional terms again shows similar behavior as the PFP theory (Figure 10b); Λ of this system depends only slightly on concentration.

Now, the occurrence of an LCST is generally attributed to differences in the free volume between the two components. In the PFP theory, this is expressed by the parameter τ, which is a measure of the differences of the reduction temperatures of the components. The reduction temperatures can be calculated by eq 4 from the reduced volumes, which in turn are a measure of free volume.

From eq 18 it can be seen that the reduction temperatures of the SL theory also depend on the reduced volume. Therefore, they are a measure of free volume as well. By inspection of the free volume term of Λ for the special case of $\Phi_1 = \Phi_2$, $\nu = 1$, and ${r_1}^0 = {r_2}^0$, it can be easily seen that it contains a factor $(T^*_1 - T^*_2)$.[2] This means that this term vanishes when both components have the same free volume, as is the case in the PFP theory. Hence, the occurrence of LCST behavior in the SL theory is also due to differences in free volume. The parameter τ in the PFP theory and λ_{12} in the SL theory play similar roles.

It even can be shown, that for the above special case (also for nonvanishing pressure) the stability conditions of the PFP and the SL theory can be put into analytically similar forms.[16] The free-volume terms contain quantities such as expansion coefficients, compressibilities, and the heat capacity C_p which are predicted similarly by both theories. Moreover, the interactional terms are proportional to $1/\tilde{v}\tilde{T}$ for both theories. Therefore, the similar behavior exhibited by both theories might be expected.

Conclusions

In this paper, the results of model calculations obtained by using the PFP theory and the SL theory are compared. These calculations reveal that despite their entirely different foundations, the predictions of both models are surprisingly similar. Not only is the phase behavior as a function of temperature described similarly by both models, but they also predict similar reasons for this behavior. The rôle played by enthalpic effects and effects of free volume is the same for both models. This is demonstrated by a comparison of the Patterson χ parameter and the parameter Λ introduced for the SL theory.

However, there are also some differences. The most obvious difference is the fact that the chain length explicitly enters into the EOS of the SL theory, while for the PFP theory there is a universal EOS, valid for all chain lengths. The fact that the latter is independent of chain length requires different reduction parameters for different chain lengths, since the variables of state of polymers depend on the degree of polymerization. Especially for very short polymers, the variables of state deviate appreciably from those of long polymers. This dependence of the state variables on chain length is predicted at least qualitatively correctly by the SL theory. However, the predicted effect is much too small. Hence, also for this theory, the reduction parameters for low molecular weight polymers have to be determined separately.

Another difference is found by comparing the parameters χ and Λ. The parameter Λ depends on composition, whereas the parameter χ does not. The latter is due to the fact, that the PFP theory is derived from a series expansion, where higher order terms are neglected. So, this theory would in fact predict a composition dependence of χ. In addition, the parameter Λ also depends on chain length. These differences lead to different shapes of phase diagrams for the two theories.

The reduction parameters used for the calculations were determined by calculating them for $p = 0$. Another possibility of determination would be a least-squares fit of the EOS to the PVT data. However, these parameters differ appreciably from the others, and by using them, the close agreement of the theories vanishes. Moreover, one finds for the parameters calculated for $p = 0$, that the ratios $(p^*_{PF}/p^*_{SL}, v^*_{PF}/v^*_{SL}, T^*_{PF}/T^*_{SL})$ (index PF and SL indicate the corresponding theory) are nearly the same for all polymers. This is not true however, for the parameters determined by a least-squares fit.

This indicates that by calculating the theoretical parameters from pure-component properties for the two theories gives agreement, whereas the model parameters obtained from a fitting procedure are not in agreement.

As the examples of PS/PMPS and PS/PCHMA show, the EOS theories are not capable of predicting phase behavior of polymer blends. Usually, one parameter has to be fitted to experimental data. Furthermore, the fact that the values of the reduction parameters—and hence the predicted phase behavior—depend on how they are determined, introduces an additional uncertainty.

Acknowledgment. We are grateful to C. Schwarzwälder for providing the poly(cyclohexyl methacrylate) and to S. Stückler for providing the polyisoprene and the polystyrene 2.1.

References and Notes

(1) Flory, P. J. *Principles of Polymer Chemistry*; Cornell University Press: Ithaca, NY, 1953.
(2) Prigogine, I. *The Molecular Theory of Solutions*; North-Holland Publishing Co.: Amsterdam, 1959.
(3) Eyring, H.; Hirschfelder, J. O. *J. Phys. Chem.* **1937**, *41*, 249.
(4) Flory, P. J.; Orwoll, R. A.; Vrij, A. *J. Am. Chem. Soc.* **1964**, *86*, 3507.
(5) Flory, P. J. *J. Am. Chem. Soc.* **1965**, *87*, 1833.
(6) Patterson, D. *J. Polym. Sci., Part C* **1968**, *16*, 3379.
(7) Sanchez, I. C.; Lacombe, R. H. *J. Phys. Chem.* **1976**, *80*, 2352.
(8) Lacombe, R. H.; Sanchez, I. C. *J. Phys. Chem.* **1976**, *80*, 2568.
(9) Zoller, P.; Bolli, B.; Pahud, V.; Ackerman, H. *Rev. Sci. Instrum.* **1976**, *49*, 948.
(10) Ougizawa, T.; Dee, G. T.; Walsh, D. J. *Macromolecules* **1991**, *24*, 3834.
(11) Patterson, D.; Robard, A. *Macromolecules* **1978**, *11*, 690.
(12) Kressler, J.; Higashida, N.; Shimomai, K.; Inoue, T.; Ougizawa, T. *Macromolecules* **1994**, *27*, 2448.
(13) Walsh, D. J.; Dee, G. T.; Halary, J. L.; Ubiche, J. M.; Millequant, M.; Lesec, J.; Monnerie, L. *Macromolecules* **1989**, *22*, 3395.
(14) Dee, G. T.; Walsh, D. J. *Macromolecules* **1988**, *21*, 815.
(15) Nishimoto, M.; Keskkula, H.; Paul, D. R. *Macromolecules* **1990**, *23*, 3633.
(16) Rudolf, B., to be published.

MA946363Z